

# Development of Multisensory Convergence in the *Xenopus* Optic Tectum

Katherine E. Deeg, Irina B. Sears and Carlos D. Aizenman

*J Neurophysiol* 102:3392-3404, 2009. First published 30 September 2009; doi:10.1152/jn.00632.2009

**You might find this additional info useful...**

---

This article **cites** 50 articles, 18 of which can be accessed free at:

</content/102/6/3392.full.html#ref-list-1>

This article **has been cited by** 3 other HighWire hosted articles

**The horizontal brain slice preparation: a novel approach for visualizing and recording from all layers of the tadpole tectum**

Ali S. Hamodi and Kara G. Pratt

*J Neurophysiol*, January 1, 2015; 113 (1): 400-407.

[\[Abstract\]](#) [\[Full Text\]](#) [\[PDF\]](#)

**Modeling human neurodevelopmental disorders in the *Xenopus* tadpole: from mechanisms to therapeutic targets**

Kara G. Pratt and Arseny S. Khakhalin

*Dis. Model. Mech.*, September , 2013; 6 (5): 1057-1065.

[\[Abstract\]](#) [\[Full Text\]](#) [\[PDF\]](#)

**Visual Experience-Dependent Maturation of Correlated Neuronal Activity Patterns in a Developing Visual System**

Heng Xu, Arseny S. Khakhalin, Arto V. Nurmikko and Carlos D. Aizenman

*J. Neurosci.*, June 1, 2011; 31 (22): 8025-8036.

[\[Abstract\]](#) [\[Full Text\]](#) [\[PDF\]](#)

**Updated information and services** including high resolution figures, can be found at:

</content/102/6/3392.full.html>

**Additional material and information** about *Journal of Neurophysiology* can be found at:

<http://www.the-aps.org/publications/jn>

---

This information is current as of April 8, 2015.

## Development of Multisensory Convergence in the *Xenopus* Optic Tectum

Katherine E. Deeg, Irina B. Sears, and Carlos D. Aizenman

Department of Neuroscience, Brown University, Providence, Rhode Island

Submitted 20 July 2009; accepted in final form 28 September 2009

**Deeg KE, Sears IB, Aizenman CD.** Development of multisensory convergence in the *Xenopus* optic tectum. *J Neurophysiol* 102: 3392–3404, 2009. First published September 30, 2009; doi:10.1152/jn.00632.2009. The adult *Xenopus* optic tectum receives and integrates visual and nonvisual sensory information. Nonvisual inputs include mechanosensory inputs from the lateral line, auditory, somatosensory, and vestibular systems. While much is known about the development of visual inputs in this species, almost nothing is known about the development of mechanosensory inputs to the tectum. In this study, we investigated mechanosensory inputs to the tectum during critical developmental stages (stages 42–49) in which the retinotectal map is being established. Tract-tracing studies using lipophilic dyes revealed a large projection between the hindbrain and the tectum as early as stage 42; this projection carries information from the Vth, VIIth, and VIIIth nerves. By directly stimulating hindbrain and visual inputs using an isolated whole-brain preparation, we found that all tectal cells studied received both visual and hindbrain input during these early developmental stages. Pharmacological data indicated that the hindbrain-tectal projection is glutamatergic and that there are no direct inhibitory hindbrain-tectal ascending projections. We found that unlike visual inputs, hindbrain inputs do not show a decrease in paired-pulse facilitation over this developmental period. Interestingly, over this developmental period, hindbrain inputs show a transient increase followed by a significant decrease in the  $\alpha$ -amino-3-hydroxyl-5-methyl-4-isoxazolepropionate (AMPA)/N-methyl-D-aspartate (NMDA) ratio and show no change in quantal size, both in contrast to visual inputs. Our data support a model by which fibers are added to the hindbrain-tectal projection across development. Nascent fibers form new synapses with tectal neurons and primarily activate NMDA receptors. At a time when retinal ganglion cells and their tectal synapses mature, hindbrain-tectal synapses are still undergoing a period of rapid synaptogenesis. This study supports the idea that immature tectal cells receive converging visual and mechanosensory information and indicates that the *Xenopus* tectum might be an ideal preparation to study the early development of potential multisensory interactions at the cellular level.

### INTRODUCTION

The optic tectum is a midbrain structure that in amphibians and other vertebrates is primarily responsible for transforming visual input into orienting behavior (Ewert 1997; Ingle 1976). Much like its mammalian homologue, the superior colliculus, the optic tectum also receives inputs from a variety of different sensory modalities, including a range of mechanosensory inputs carrying somatosensory, auditory, vestibular, and lateral-line information (Behrend et al. 2006; Lowe 1986, 1987; Munoz et al. 1995; Vanegas 1984). In the colliculus, convergence between different sensory inputs can lead to multisensory integration, a process important for enhancing detection, localization, identification, and response to external environmental events (for a review, see Stein et al. 2009). In the

tectum, however, it is not as well understood how the convergence of the different sensory modalities leads to multisensory integration nor how these properties emerge during early development. Normal development of multisensory properties of tectal and collicular neurons, at least in some species, is known to depend on early sensory experience (Knudsen 2002; Wallace and Stein 2007; Wallace et al. 2006); however, the details of this developmental process are poorly understood at the cellular level. It is also not clear whether this is a general principle that applies to all vertebrates. To better understand these processes in the tectum, it is necessary first to understand how inputs from different sensory modalities begin to converge onto tectal neurons during early development.

In *Xenopus*, as well as in other vertebrates, the dominant input to the optic tectum is visual and originates from the contralateral retina, terminating within the superficial layers of the tectal neuropil (Székely and Lázár 1976). Inputs from the various mechanosensory modalities, in contrast, terminate within the deeper layers (Behrend et al. 2006; Lowe 1986, 1987; Munoz et al. 1995). In adult *Xenopus*, auditory and lateral-line inputs reach the tectum both via the torus semicircularis, a structure analogous to the mammalian inferior colliculus (Will et al. 1985a,b; Zittlau et al. 1988), and from direct inputs from medullary nuclei in the hindbrain that receive VIIIth (dorsal medullary nucleus) and lateral-line (lateral line nucleus) nerve inputs (Lowe 1986; Will et al. 1985a,b). Somatosensory inputs also innervate the deeper layers of the frog tectum (Munoz et al. 1995; Tsurudome et al. 2005). One route is via ascending inputs from the dorsal column nucleus in the hindbrain that receives inputs from various primary somatosensory ganglia including the trigeminal ganglion (Munoz et al. 1995; Tsurudome et al. 2005). Trigeminal inputs also reach the tectum via mesencephalic trigeminal cells (Hiscock and Straznicky 1982; Lowe and Russell 1984).

While many of these ascending sensory pathways are present in adult *Xenopus* and during late larval stages (Nieuwkoop-Faber stages 56–60) (Chahoud et al. 1996), there is evidence that they may arise much earlier (Hiramoto and Cline 2008; Pratt and Aizenman 2009). Also it is not clear at which point in development they begin to make functional synapses onto tectal neurons. Although the early functional and anatomical development of visual inputs to the tectum has been well characterized (Aizenman and Cline 2007; Akerman and Cline 2006; Dong et al. 2009; Pratt and Aizenman 2007; Ruthazer et al. 2003; Tao and Poo 2005; Wu et al. 1996; Zou and Cline 1999), much less is known about the development of nonvisual modalities that project to the tectum. Visual inputs begin to innervate the tectum around developmental stage 39 and functional synapses can be recorded around stage 41 (Holt 1989; Zhang et al. 1998). Between stages 42 and 49, the visual projection undergoes dramatic activity-dependent anatomical

Address for reprint requests and other correspondence: C. D. Aizenman, Dept. of Neuroscience, Box G-LN, Brown University, Providence, RI 02912.

and electrophysiological changes as the retinotectal map becomes refined (Akerman and Cline 2006; Cline et al. 1997; Dong et al. 2009; Pratt and Aizenman 2007; Pratt et al. 2008; Tao and Poo 2005). During this time, anatomical studies indicate that mechanosensory inputs from the Vth and VIIIth nerves also project to the tectum via primary sensory nuclei in the hindbrain (Tsurudome et al. 2005). Electrophysiological recordings also show that somatosensory inputs originating from the mouth area can be recorded from stage 49 tectal neurons (Pratt and Aizenman 2009). This suggests that some mechanosensory modalities may begin to innervate the tectum almost as early as visual inputs do, but the details are yet to be elucidated. Typically, multisensory neurons in the tectum and superior colliculus in various species are found in deeper layers; however, during early *Xenopus* tadpole development (stages 42–49), cells from the various tectal layers have not yet fully differentiated (Lazar 1973); therefore it is also unclear whether the organization of multisensory neurons in the young tadpole will differ significantly from that in adults.

To begin to address these questions, in this study, we describe for the first time the functional development of mechanosensory synapses to the optic tectum during a time period in which the retinotectal map is being established and refined. We have developed a preparation in which we can independently activate visual and mechanosensory inputs to the optic tectum by directly stimulating, respectively, the optic chiasm and a combination of primary sensory nuclei in the hindbrain in an isolated tadpole brain. Here, we characterize the hindbrain-tectal projection between a range of developmental stages (stages 42–49) during which the retinotectal map is being established and refined. We describe the synaptic properties of mechanosensory inputs to tectal cells and elucidate developmental differences between projections carrying visual and nonvisual information. Our study shows that multisensory integration is present very early on in development, and establishes the *Xenopus* tadpole as a useful model system by which to study the role of experience in the development of multisensory convergence.

## METHODS

### Dye injection and imaging

All experiments were conducted in accordance with Institutional Animal Care and Use Committee (IACUC) guidelines. *Xenopus laevis* tadpoles were reared in 10% Steinberg's solution under 12-h light/dark cycles at 21°C. Animals were staged according to Nieuwkoop and Faber (1956). Under our rearing conditions, animals reached stage 42–43 ~7–9 days post fertilization (dpf), stage 44–46 by 9–12 dpf, and stage 48–49 at 17–20 dpf. Animals were anesthetized in 0.01% tricaine methanesulfonate MS-222 (Sigma) dissolved in Steinberg's solution, then fixed for a minimum of 24 h in 4% paraformaldehyde in phosphate buffer, pH 7.4 at 4°C. Fine glass micropipettes were filled with solutions of 2% 1,1'-dioctadecyl-3,3,3',3'-tetramethylindocarbocyanine perchlorate (DiD, Molecular Probes) in ethanol and injected intraocularly using a Pressure System IIe (Toohey) pressure injector to completely fill the contralateral eye. Micropipettes containing 0.2% 1,1'-dioctadecyl-3,3,3',3'-tetramethylindocarbocyanine perchlorate (DiI, Molecular Probes) in ethanol were injected into the contralateral trigeminal ganglion, the VIIth and VIIIth nerve bundle, or the hindbrain region to release a small amount of dye. Tadpoles were incubated at room temperature for 4 days for dye transport. This was sufficient time for the dye to fully reach the fiber terminals.

Confocal z-series (12-bit data) of the labeled projections were collected using a Zeiss LSM-510 confocal microscope with a  $\times 10$  or  $\times 20$  objective. To generate the fluorescence maps in Fig. 2, a region of interest (ROI) in the tectal neuropil was selected that encompassed the terminal areas of both projections (Fig. 2A). The ROI was aligned along the rostrocaudal axis. At each optical slice, the fluorescence value for each fluorescence channel was averaged across the ROI and displayed as a single trace. Thus each trace represents the average fluorescence across the rostrocaudal axis at different depths, starting from dorsal (top) and going to ventral (bottom). This allows us to display the fluorescence value at different depths for both projections separately. To display total overlap in the rostrocaudal axis (Fig. 2D), all fluorescence traces from all z-values were averaged and normalized. Using this technique only tells us the degree to which hindbrain and visual inputs overlap in a given region along the rostrocaudal axis but does not imply that the inputs occupy the same region of three dimensional space as they may be in different layers, as indicated in the fluorescence maps described above. Image analysis was performed using Image-J software. All conditions were done, at minimum, in triplicate to confirm that the data were representative.

### Whole cell electrophysiology

The whole-brain preparation used in these experiments was prepared as previously described (Pratt and Aizenman 2007; Wu et al. 1996). Briefly, tadpoles were anesthetized in 0.01% MS-222. To expose the ventral surface of the tectum, the brains were filleted along the dorsal midline and dissected out of the animal in HEPES-buffered extracellular saline (containing, in mM: 115 NaCl, 4 KCl, 3 CaCl<sub>2</sub>, 0.5 MgCl<sub>2</sub>, 5 HEPES, 10 glucose, 0.1 picrotoxin, pH 7.2, 255 mosM). The whole-brain preparation was pinned to a submerged silicone elastomer (Sylgard, Dow Corning, Midland, MI) block in a custom-made recording chamber. The ventricular membrane overlying the tectal cells was carefully removed with a broken glass micropipette. Individual tectal cells were resolved using a Nikon E600 FN light microscope (Tokyo) with a  $\times 60$  fluorescent water-immersion objective and a Hamamatsu (Hamamatsu City, Japan) infrared (IR) CCD camera. Recordings were made at ambient room temperature (20–22°C).

Synaptic responses were evoked using bipolar stimulating electrodes (FHC, No. CE2C7S) placed in the optic chiasm and/or the contralateral hindbrain. A 0.2-ms shock was administered at varying stimulus intensities to elicit a tectal response. With the exception of graded stimulation experiments, stimulus intensity was set so as to evoke a monosynaptic tectal cell response with minimal confounding polysynaptic activity. A minimum of 10 trials was averaged for each given stimulus intensity in a specific experiment. Tectal responses were recorded in whole cell voltage-clamp mode using glass micropipettes (8–12 M $\Omega$ ) filled with potassium gluconate-based intracellular saline (containing, in mM: 100 potassium gluconate, 8 KCl, 5 NaCl, 1.5 MgCl<sub>2</sub>, 20 HEPES, 10 EGTA, 2 ATP and 0.3 GTP, pH 7.2, 255 mosM). For Sr<sup>2+</sup> experiments, 3 mM Sr<sup>2+</sup> was substituted for external Ca<sup>2+</sup>. Unless otherwise stated, all experiments were performed in the presence of 1 mM picrotoxin (PTX). All chemicals were obtained from Sigma-Aldrich. To eliminate variations in tectal neuron maturity due to the developmental gradient (Wu et al. 1996), recordings were performed on neurons in the middle third of the tectum (Akerman and Cline 2006; Pratt and Aizenman 2007). Signals were measured with a Multiclamp 700B amplifier (Axon Instruments), digitized at 10 kHz using a Digidata 1322A A-D board and acquired using P-Clamp 9 software. Membrane potential in the figures was not adjusted to compensate for the predicted 12 mV liquid junction potential. After (Clements and Bekkers 1997), spontaneous, and evoked synaptic events were collected and quantified through the use of a variable amplitude template, which was determined for every experiment from averaged events. The templates detected events with a minimum of 10-ms separation between peaks and were therefore



stringent enough to exclude overlapping events. AxographX software (Axon Instruments) was used to analyze data. InStat by GraphPad Software was used to calculate statistics. Unless otherwise specified, all statistics are nonparametric. To test differences in paired-pulse and AMPA/N-methyl-D-aspartate (NMDA) ratios, and in asynchronous excitatory postsynaptic potential (aEPSC) amplitude across development we used a Kruskal-Wallis test with a Dunn's multiple comparisons posttest. To test for differences between hindbrain and visual aEPSC amplitudes within a given stage, we used a Wilcoxon matched-pairs test. All error bars are SE.

### Pharmacology

NMDA receptors were blocked with 50  $\mu$ M D-(–)-2-amino-5-phosphonopentanoic acid (D-AP5), a competitive NMDA receptor antagonist. The  $\alpha$ -amino-3-hydroxy-5-methyl-4-isoxazole propionic acid (AMPA) receptors were blocked with 20  $\mu$ M of the competitive antagonist 2,3-dioxo-6-nitro-1,2,3,4-tetrahydrobenzo[f]quinoxaline-7-sulfonamide (NBQX). Both D-AP5 and NBQX were obtained from Tocris Bioscience. To assess the nature of inhibitory projections to the tectum, we blocked AMPA and NMDA receptors (AMPA and NMDARs) as described in the preceding text and stimulated the hindbrain in the absence of PTX. These evoked inhibitory currents were measured at +5 mV from individual tectal neurons.

### Data analysis

Paired-pulse facilitation (PPF), AMPA/NMDA ratios, and responses to graded stimulation were all measured using the normal intracellular solution described in the preceding text. To measure quantal sizes, 3 mM  $\text{Sr}^{2+}$  was substituted for external  $\text{Ca}^{2+}$ . For all tests of synaptic development, stimulus intensities ranged between 0.01 and 0.5 mA. Paired-pulse responses were elicited at –60 mV with an interstimulus interval (ISI) of 100 ms. A minimum of 10 trials was averaged for each cell. The amount of facilitation for each cell was determined by calculating the peak AMPA amplitude ratio of response 2/response 1 (after Akerman and Cline 2006) to stimuli pairs. The amount of facilitation per stage epoch was determined by averaging the amount of facilitation for each cell from animals within that developmental stage range.

The AMPA/NMDA ratios were calculated according to Wu et al. (1996). Briefly, measured AMPAR-mediated EPSCs recorded at –60 mV were compared with NMDAR-mediated EPSCs recorded at +60 mV. A minimum of 10 trials was recorded at each potential. Stimulus intensities varied between cells but were sufficient to produce a reliable, monosynaptic response with minimal confounding polysynaptic activity. Transmission failures were included in the averages. To calculate the A/N ratio for each cell, the average peak AMPA response was divided by the averaged NMDAR-mediated response, which was the averaged amplitude between 20 and 30 ms post-response onset. At this time window, the AMPA component has decayed to <10% of the peak value. The A/N ratio for each developmental epoch was determined by averaging the A/N ratios for each cell within each of the three stage ranges.

To assess the relative number of fibers composing the hindbrain-tectal projection, we measured the evoked current in response to a range of stimulus intensities. Minimum stimulation was defined as the stimulus intensity that resulted in a transmission failure ~50% of the time. Maximum stimulation was defined as the stimulus intensity beyond which the response amplitude will not increase. Minimum and maximum stimulation intensities were determined for each cell. To determine the graded nature of hindbrain-tectal responses, each cell was stimulated at a minimum of three stimulus intensities between the experimentally determined minimum and maximum starting slightly below minimum. Normalized response amplitudes were plotted against normalized stimulus intensities for each cell. Cells were grouped according to developmental stage.

To determine the quantal size of hindbrain- and retino-tectal inputs, we substituted 3 mM  $\text{Sr}^{2+}$  for external  $\text{Ca}^{2+}$ . To ensure that the events we measured were due to hindbrain stimulation and not spontaneous, we excluded traces where the number of events in the 125 ms preceding the stimulus onset was >25% of the events seen in the first 125 ms poststimulus. Amplitudes of detected events were averaged across cells and then across stages.

InStat by GraphPad Software was used to calculate statistics. All statistics are nonparametric. To test differences in paired-pulse and AMPA/NMDA ratios, and in aEPSC amplitude across development, we used a Kruskal-Wallis test with a Dunn's multiple comparisons posttest. To test for differences between hindbrain and visual aEPSC amplitudes within a given stage, we used a Wilcoxon matched-pairs test. All error bars are SE.

## RESULTS

### Tracing of mechanosensory inputs

While much is known about the development of the retino-tectal projection (Akerman and Cline 2006; Pratt and Aizenman 2007; Tao and Poo 2005)—the primary sensory input to the tectum—almost nothing is known about the development of projections that carry nonvisual sensory information to the tectum. To test whether these nonvisual projections are present in the tectum during key early developmental stages, we first performed a series of tract-tracing experiments on stage 49 tadpoles. Mechanosensory information originating from somatosensory, lateral line and auditory systems is known to project to the tectum via their primary sensory nuclei in the hindbrain. In this study, we traced these pathways anterogradely in tadpoles using lipophilic dyes (DiI and/or DiD). We injected these dyes directly into the trigeminal ganglion (Fig. 1A) and the more posterior nerve bundle carrying the VII (facial), VIII (acousticovestibular), and lateral line nerves (Fig. 1B). We found that these nerve bundles all project ipsilaterally into the hindbrain. On entering the hindbrain, both projections split, sending fibers both rostrally and caudally (Fig. 1, A and B). The terminal arborizations of these projections terminate in areas corresponding to primary sensory nuclei, but due to the small size of the tadpole brain, completely separate terminal areas could not be discerned for the different nerve bundles. In separate experiments, dye injection into the hindbrain in the area where the primary afferents terminate shows a substantial projection to the contralateral tectum. This confirms that direct inputs projecting from primary mechanosensory nuclei in the hindbrain to the tectum are present during early development (Fig. 1, C and D).

To directly compare the development of these mechanosensory pathways in relation to visual input, we injected DiI and DiD into the eye and the hindbrain, respectively, of other tadpoles at stages 42, 45, and 49. We chose these developmental stages because the retinotectal projection has been well characterized during this time and is known to undergo significant change, allowing us to make direct comparisons between what is known about the developing retinotectal projection with our data concerning the hindbrain-tectal projection. Because both retinal and mechanosensory inputs are known to be organized in topographically aligned maps, knowing how mechanosensory and visual inputs interact during this period will ultimately be useful for understanding how these maps become aligned. During stage 42, the retinal afferents are very immature and begin to make functional synapses within the

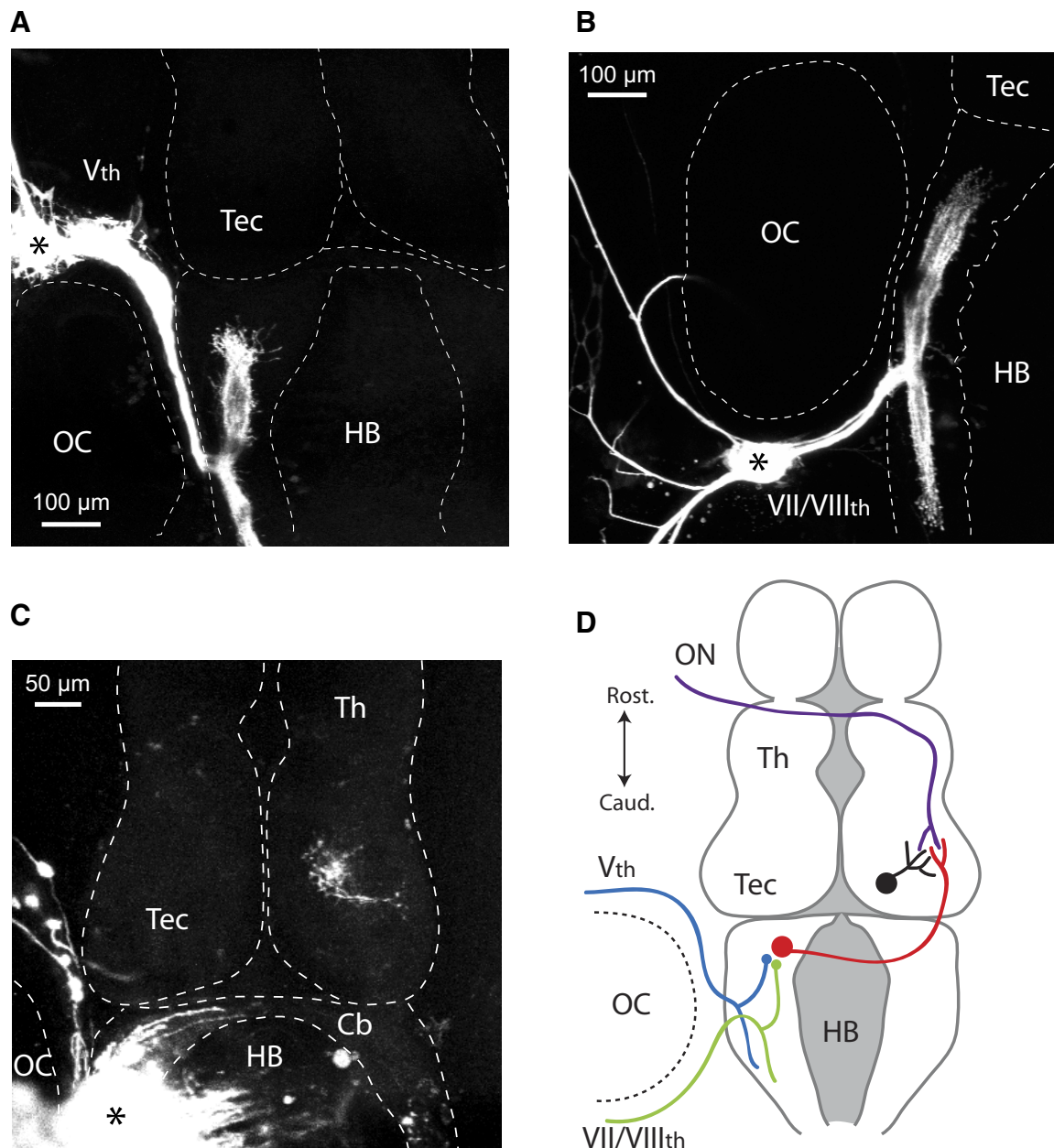


FIG. 1. Mechanosensory inputs to the tectum. *A*: 1,1'-diiodo-3,3',3'-tetramethylindocarbocyanine perchlorate (DiI) injection into the trigeminal ganglion (Vth nerve). After entering the hindbrain the projection terminates rostrally and caudally in the ipsilateral hindbrain. *B*: DiI injection into the posterior nerve bundle carrying the facial (VIIth), acoustico-vestibular (VIIIth), and lateral-line nerves, reveals that projections also terminate in the rostral and caudal regions of the ipsilateral hindbrain. *C*: dye injection into the hindbrain shows a projection from the termini of primary sensory afferents to the contralateral tectum. *D*: schematic summarizing the input composing the hindbrain-tectal projection. The Vth, VIIth, and VIIIth nerves terminate on primary sensory nuclei in the ipsilateral hindbrain. The hindbrain-tectal projection arises from these primary sensory nuclei and travels to the contralateral tectum where it makes synapses with individual tectal neurons that also receive direct visual input from the retina. ON, optic nerve; Th, thalamus; Tec, tectum; HB, hindbrain; Cb, cerebellum; OC, otic capsule. \*, injection site. All injections were done at least in triplicate. Images are maximal projections of confocal stacks. Orientation of images is the same as in *D*.

tectum. Between stage 45 and 49, there is a massive increase in activity-dependent dendritic growth and synaptogenesis, synaptic maturation, and plasticity of the retinotectal pathway. All these changes result in refinement of the retinotectal map and shrinking of visual receptive fields (Akerman and Cline 2006; Dong et al. 2009; Pratt and Aizenman 2007; Tao and Poo 2005).

We found that the tectum is innervated by both sets of inputs during all three stages (Fig. 2A). During these stages, the

hindbrain-tectal projection appears to become increasingly dense, although this is difficult to quantitate due to variability in dye injection. While the hindbrain and visual projections terminate in the same region of the tectal neuropil, hindbrain projection inputs terminate deeper than the visual projection (Fig. 2, B–D). The adult tectum is layered into multiple laminae that receive inputs from the various sensory modalities (Székely and Lázár 1976). In the tadpole, the tectum is composed of only two layers, the neuropil layer, and the cell body

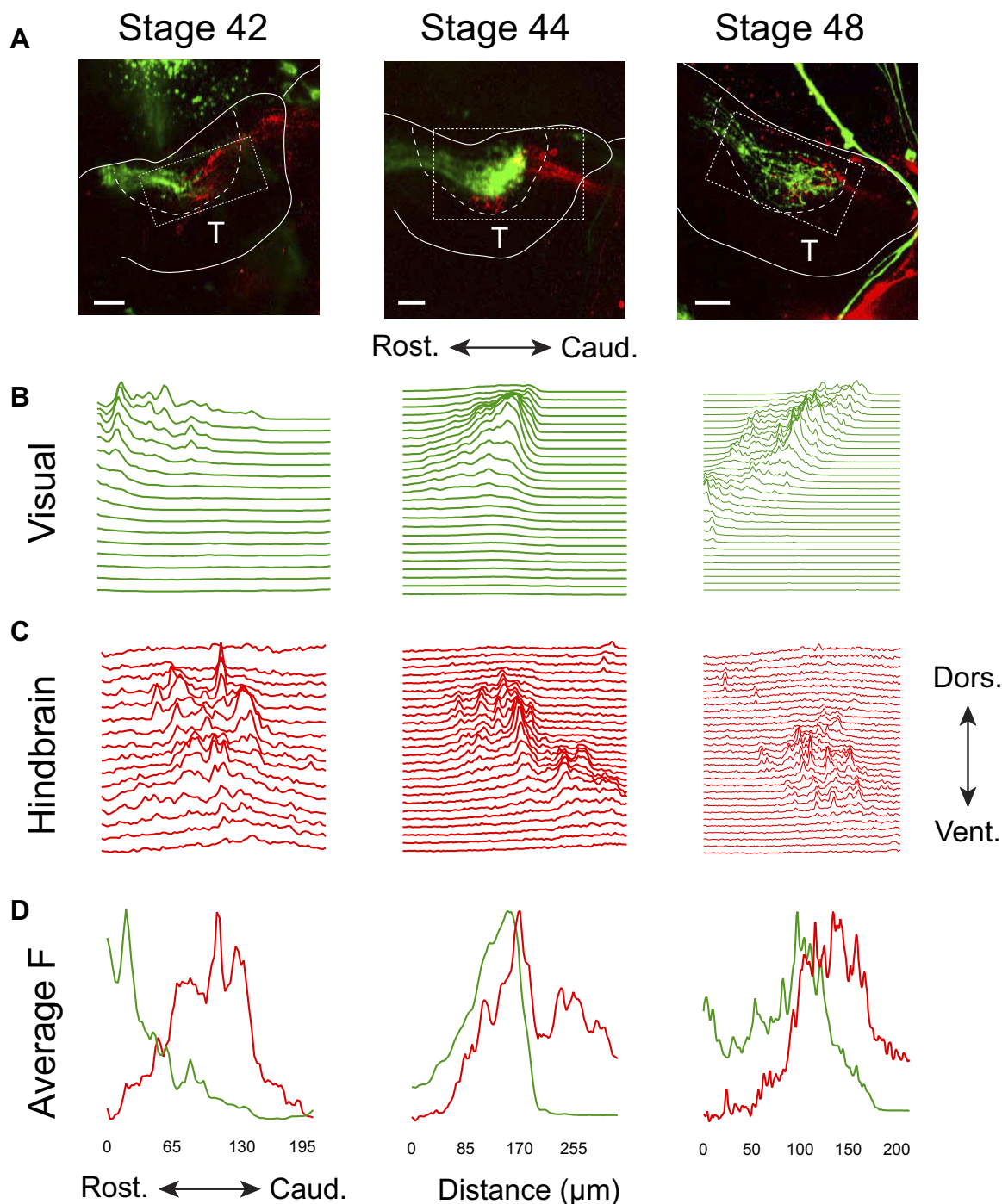


FIG. 2. Development of convergence of hindbrain and visual inputs to the tectum. *A*: maximal projection of a confocal z-series for visual (green) and hindbrain (red) inputs to the tectum at different developmental stages. Each tectal lobe receives a projection from the eye and the hindbrain, which carry visual and mechanosensory information, respectively. These projections are present at all 3 developmental stages investigated here. —, the tectum outline. - - -, the tectal neuropil. Black box represents the region of interest used in *B–D*. Scale bars are 50  $\mu\text{m}$ . *B* and *C*: normalized fluorescence values collected across the region of interest in the tectum indicated in *A* for the 2 different fluorescence channels representing visual and hindbrain projections. Fluorescence was averaged in the rostrocaudal axis. Each trace represents the fluorescence profile at a given depth (see METHODS). z-stacks were collected every 7.5  $\mu\text{m}$  in the stage 42 and 44 tecta and at every 4  $\mu\text{m}$  in the stage 48 tectum. Notice that the hindbrain projection terminates at a deeper layer than does the visual projection. *D*: averaged fluorescence for each channel at all depths across the rostrocaudal axis. This shows that even at stage 42, visual and hindbrain inputs overlap in the rostrocaudal direction in the tectum. Images are representative animals from each of the developmental stages. All injections at each stage were done at least in triplicate. T, tectum.

layer. Dendrites of tectal neurons are known to span the entire neuropil layer in the ventral to dorsal direction (Lazar 1973; Wu and Cline 1998, 2003) (Fig. 3, *A* and *B*). This suggests that individual tectal neurons may receive inputs from both visual

and mechanosensory inputs. The observation that hindbrain inputs terminate deeper (more dorsal) within the tectal neuropil also suggests that mechanosensory inputs terminate closer to the tectal cell soma than the visual inputs. Thus as in adult



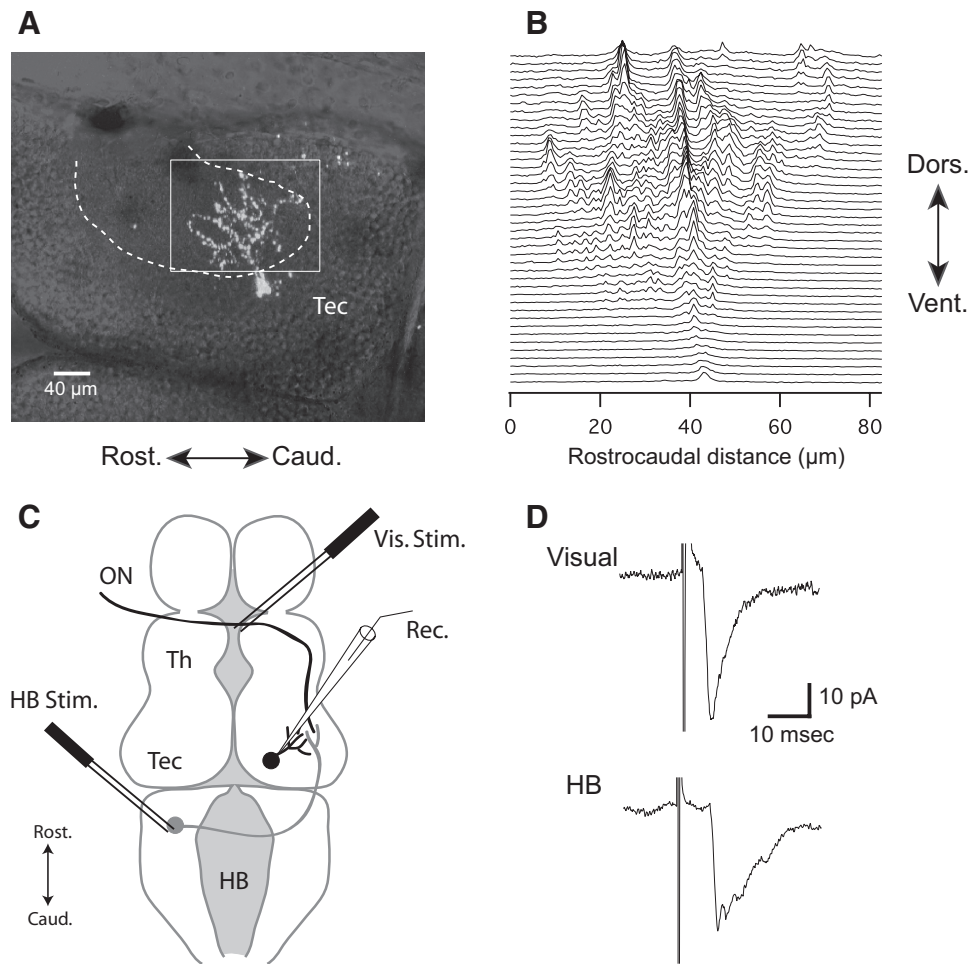


FIG. 3. Tectal neurons receive both hind-brain and visual input. *A*: maximal projection of a confocal  $z$ -series of a stage 49 tectal neuron labeled with FITC-dextran. Projection is superimposed on a single optical plane of the transmitted light image to show the relationship of the neuron's dendritic arbor relative to the neuropil layer. ---, border between cell body layer and the neuropil. Black box represents the region in which the fluorescence profiles in *B* were measured. *B*: normalized fluorescence values collected across the region of interest in the tectum indicated in *A*. Fluorescence was averaged in the rostrocaudal axis. Each trace represents the fluorescence profile at a given depth (see METHODS).  $z$ -stacks were collected every 1.6  $\mu\text{m}$ . Notice that the dendritic arbor spans almost all entire neuropil region in the ventral to dorsal axis and overlaps with the termination depths of both hindbrain and visual inputs. *C*: schematic of stimulation and recording configuration for electrophysiological experiments. Mechanosensory pathways are activated by electrically stimulating the hindbrain, while visual inputs are activated by stimulating the optic nerve at the optic chiasm. Whole cell voltage-clamp recordings were performed from individual tectal neurons. *D*: monosynaptic responses could be evoked by either stimulating the hindbrain or visual inputs. All cells in which visual inputs could be evoked also had hindbrain-evoked responses and vice versa.

animals, the two projections are segregated to different layers within the tectal neuropil even if the tectal laminae are not fully differentiated at these early stages (Lazar 1973). Furthermore, the layering of the sensory projection appears to be present from the very earliest stages studied.

Taken together, our data are consistent with an interpretation that the hindbrain-tectal projection is present at very early stages and thus the structural capability to relay mechanosensory information is present.

#### Functional development of mechanosensory synapses in the tectum

While our anatomical data suggest that mechanosensory inputs innervate the tectum starting from at least stage 42, we do not know whether these projections—similarly to visual inputs—make functional synapses during these stages. To directly activate visual and mechanosensory pathways, we used an isolated whole-brain preparation (Wu et al. 1996) and electrically stimulated the optic chiasm and the hindbrain, while performing whole cell recordings in the contralateral tectum (Fig. 3*C*). We found that, at all stages tested, almost all neurons that received synaptic input from the optic nerve could also be directly activated by stimulating the hindbrain and vice versa (Fig. 3*D*). Due to the small size of the tadpole hindbrain and the inability to clearly distinguish between different primary sensory nuclei during these developmental stages, it is

likely that we are concurrently activating a mix of various ascending sensory fibers carrying different types of mechanosensory modalities. We performed a series of electrophysiological tests designed to characterize the development of mechanosensory input to the tectum during the range of developmental stages described in the preceding text.

We first characterized the pharmacology of synaptic transmission in this pathway. In general, excitatory synapses in the developing tectum are glutamatergic. This was confirmed when we recorded spontaneous excitatory postsynaptic currents (sEPSCs) in tectal cells and showed that these could be completely eliminated by AMPA and NMDA receptor antagonists NBQX (20  $\mu\text{M}$ ) and D-AP5 (50  $\mu\text{M}$ ; Fig. 4*A*; see METHODS). It is also known that the retinotectal projection is glutamatergic and that responses are mediated by AMPA- and NMDA-type glutamate receptors (Wu et al. 1996). We tested whether this was also true in the hindbrain-tectal projection. EPSCs in tectal cells were evoked by focally stimulating the contralateral hindbrain in the presence of PTX, a GABA<sub>A</sub>R and GABA<sub>C</sub>R antagonist, to block recurrent inhibition. Evoked responses, recorded at  $-60$  mV, were completely abolished by NBQX (20  $\mu\text{M}$ ), a competitive AMPA receptor antagonist (Fig. 4*B*). To test whether NMDARs were present, we then stimulated the hindbrain-tectal projection while depolarizing the membrane potential to  $-20$  mV to remove the  $\text{Mg}^{2+}$  block of NMDARs. At this depolarized potential, we observed a slow inward current consistent with the activation of NMDARs (Fig.

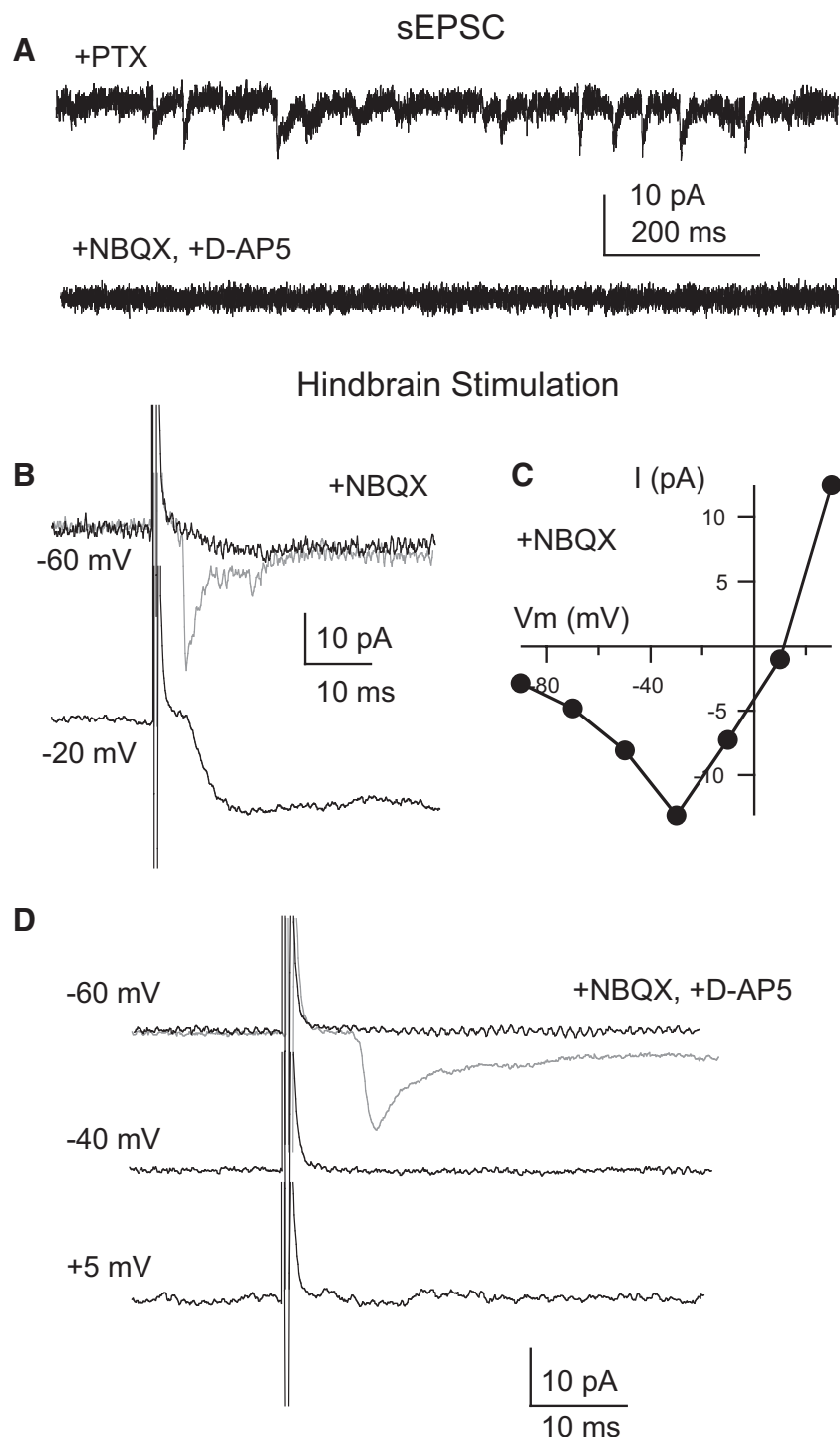


FIG. 4. Hindbrain-tectal synapses are glutamatergic. **A**: excitatory postsynaptic currents (sEPSCs) in tectal neurons are blocked by co-application of the AMPA and *N*-methyl-D-aspartate (NMDA) receptor antagonists 2,3-dioxo-6-nitro-1,2,3,4-tetrahydrobenzo[f]quinoxaline-7-sulfonamide (NBQX) and D-(−)-2-amino-5-phosphonopentanoic acid (D-AP5). **B**: in the presence of GABA receptor (GABAR) blocker PTX, the AMPAR antagonist NBQX blocks the evoked hindbrain-tectal currents at −60 mV. Depolarization of the tectal neurons to −20 mV reveals that hindbrain-tectal currents are also mediated by NMDA receptor (NMDAR). **C**: current ( $I$ )–voltage ( $V$ ) relationship at hindbrain-tectal synapses in the presence of NBQX.  $I$ – $V$  curve is voltage-dependent, consistent with the activation of NMDARs. **D**: there are no monosynaptic ascending inhibitory hindbrain-tectal connections. NBQX and D-AP5 eliminate all hindbrain-evoked synaptic transmission. Gray trace, control recording; black trace, in the presence of the drugs. The tectal neuron was depolarized to +5 mV, a potential at which inhibitory activity would be present. Stimulation of the hindbrain in the presence of these blockers reveals the absence of direct inhibitory hindbrain-tectal synapses.

4B). The current-voltage ( $I$ – $V$ ) relationship of this synaptic current further confirmed that it was mediated by NMDARs (Fig. 4C). We then tested whether any ascending projections from the hindbrain to the tectum could be inhibitory. When we blocked excitatory synapses with D-AP5 and NBQX, we were unable to detect any synaptic responses at a variety of membrane potentials, indicating the absence of any ascending inhibitory inputs in this projection (Fig. 4D). Taken together, these pharmacological data show that, like the retinotectal projection, the hindbrain-tectal synapses are excitatory and are mediated by AMPA and NMDA receptors.

To functionally characterize the development of the hindbrain-tectal projection, we measured the paired-pulse (PP) and AMPA/NMDA (A/N) ratios of developing hindbrain-tectal synapses. By measuring the amount of paired-pulse facilitation or depression, we can get an indication of the maturational state of the presynaptic terminal. Some nascent glutamatergic synapses have immature vesicle release machinery and often cannot release all of their neurotransmitter-containing vesicles in response to a single stimulus. When two stimuli are given in rapid succession, the response of immature synapses to the second stimulus is usually larger in amplitude than to the first,



resulting in paired-pulse facilitation (PPF) (Akaneya et al. 2003; Gasparini et al. 2000; Thomson 2000). Younger synapses usually facilitate in response to this protocol, resulting in a paired-pulse ratio that is  $>1$ . In retinotectal synapses, the degree of facilitation decreases significantly between stages 42 and 49 (Aizenman and Cline 2007). We found that hindbrain-tectal projections were slightly facilitating during stages 42/43 ( $1.3 \pm 0.07$ ,  $n = 7$ ), and stages 44–46 ( $1.2 \pm 0.3$ ,  $n = 11$ ) and this facilitation decreased by stages 48/49 (Fig. 5, A and B;  $1.0 \pm 0.9$ ,  $n = 11$ ). This trend, however, was not statistically significant ( $P > 0.05$ ). Thus in contrast to the retinotectal projection, hindbrain synapses do not appear to significantly change their release properties during this developmental time period. There are several possible explanations for this. One possibility is that by the time hindbrain inputs reach their targets in the tectum, they already have fairly developed release machinery or that they reach the tectum much earlier than visual synapses. Alternatively, it is possible that the various sensory modalities contained in the hindbrain projection have different release properties, leading to variability in the data.

To further characterize the maturation of the developing hindbrain-tectal projection, we measured their A/N ratio. Immature glutamatergic synapses are characterized as having primarily NMDAR (Isaac et al. 1997; Wu et al. 1996). Because NMDAR are inactive at resting membrane potentials, these synapses are functionally silent. As retinotectal synapses mature, AMPA receptors are added, rendering NMDAR-containing synapses functional (Akerman and Cline 2006; Wu et al. 1996). Thus one way to gauge the maturity of a synapse is by measuring the amount of current carried by AMPAR and comparing it with the amount of current carried by NMDAR. To measure the A/N ratio, we measured AMPAR- and NMDAR-mediated currents independently (see METHODS).

AMPA-mediated tectal cell responses were recorded in response to hindbrain stimulation at  $-60$  mV, a membrane potential at which NMDAR are blocked by  $Mg^{2+}$ . To determine the NMDAR-mediated response, we recorded evoked currents from the same neuron when it was depolarized to  $+60$  mV. Between developmental stages 42/43 and 44–46, we found that the A/N ratio increases, but this change was not statistically significant (Fig. 6, A and B; stage 42/43:  $1.45 \pm 0.3$ ,  $n = 7$ ; stage 44–46:  $2.5 \pm 0.6$ ,  $n = 11$ ). However, unlike retinotectal synapses, we found that the A/N ratio decreases significantly between stage 44–46 and 48/49 ( $1.0 \pm 0.2$ ,  $n = 15$ ,  $P = 0.0281$ ).

One possible explanation for this observed decrease in the A/N ratio is that between stages 44–6 and 48/9 a large wave of synaptogenesis occurs in the hindbrain-tectal projection. These newly formed synapses would be dominated by NMDARs, therefore decreasing the overall A/N ratio of the projection. This idea is supported by the observations that the important aspects of lateral-line mediated behavior mature around stage 47 (Simmons et al. 2004) and that the inner ear, in which auditory and vestibular inputs originate, quadruples in size between stages 45 and 50 (Quick and Serrano 2005). This restructuring in the various mechanosensory modalities that compose the hindbrain-tectal projection would result in an increase in the number of hindbrain inputs innervating the tectum. To test this prediction, we measured the response of tectal cells to graded increases in the intensity of stimulation of the hindbrain projection.

In this experiment, we first determined a minimum and maximum stimulation intensity for each cell (see METHODS). Synaptic events evoked by minimal stimulation are interpreted as being the result of the stimulation of a single axon (Liao et al. 1995; Wu et al. 1996). We generated input/output curves for each cell (Fig. 7) across a range of developmental stages by

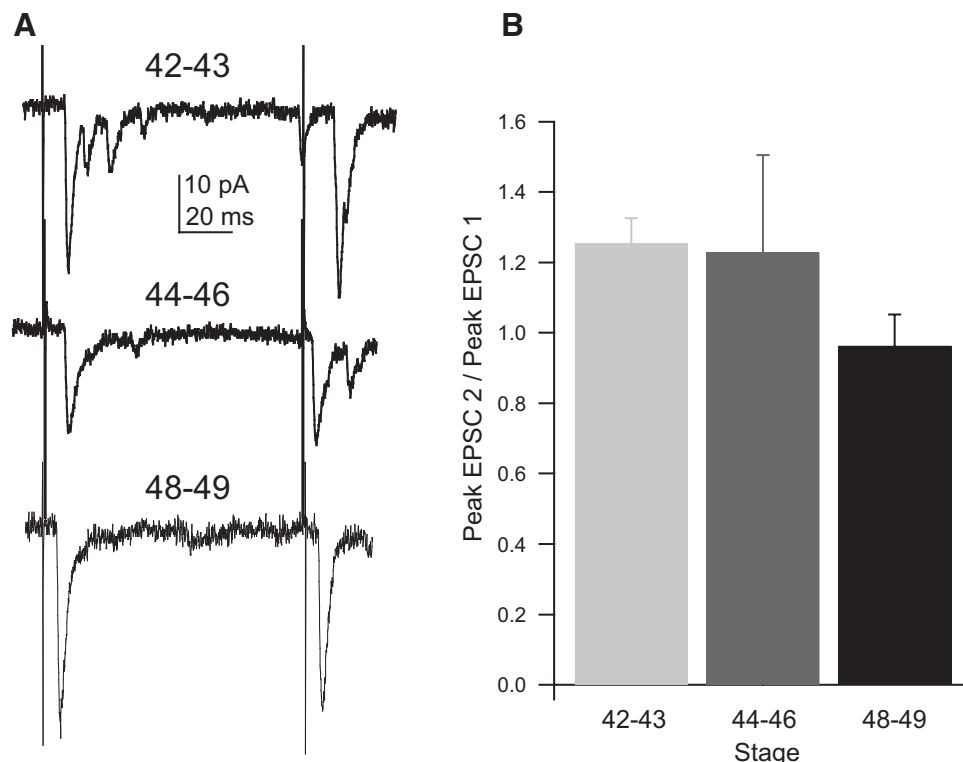


FIG. 5. There is no developmental change in paired-pulse ratio at hindbrain-tectal synapses. A: representative traces from tadpoles of each of the three stage epochs investigated, 42–43, 44–46, and 48–49. B: paired-pulse ratios expressed as the amplitude ratio between the peak values of excitatory postsynaptic currents 2 and 1 (EPSC2/EPSC1) for tadpoles from stages 42–43 ( $1.3 \pm 0.07$ ,  $n = 7$ ); 44–46 ( $1.2 \pm 0.3$ ,  $n = 11$ ); and 48–49 ( $1.0 \pm 0.9$ ,  $n = 11$ ).  $P > 0.05$ , error bars are SE.

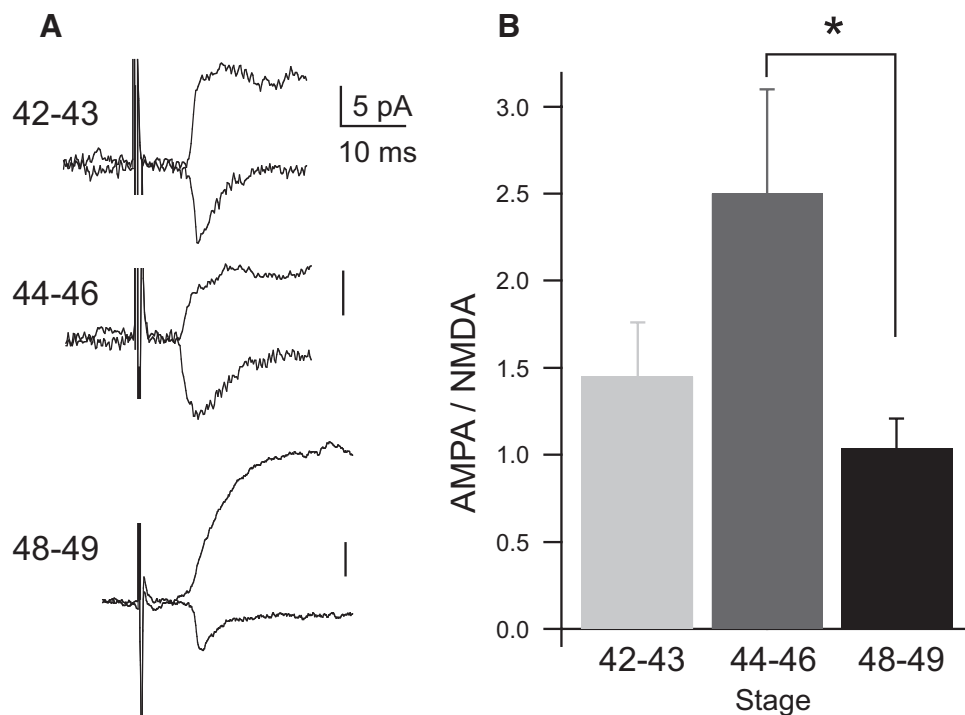


FIG. 6. The AMPA/NMDA ratio at hind-brain-tectal synapses transiently increases and then decreases during development. *A*: representative tectal responses to hind-brain stimulation recorded at  $-60$  mV and  $+60$  mV. An average of 10 traces were averaged at  $-60$  mV to represent the AMPA response and  $+60$  mV to represent the NMDA response. Traces were from the same cell and superimposed. *B*: the average A/N ratio across development beginning with stage 42 ( $1.45 \pm 0.3$ ,  $n = 7$ ) and showing a significant decrease between stage 44–46 ( $2.5 \pm 0.6$ ,  $n = 11$ ) and 48–49 ( $1.0 \pm 0.2$ ,  $n = 15$ ,  $P = 0.0281$ ). Error bars are SE. A/N ratios were calculated as indicated in methods.

plotting normalized response amplitudes against normalized stimulus intensities. If a given cell is innervated by one or a few fibers, the response amplitude will show sudden large “jumps” as the stimulus intensity is increased, whereas if the cell is innervated by multiple fibers, the response amplitude will increase in a more graded manner. Individual input-output curves were grouped according to whether they showed at least one jump in amplitude of  $\geq 65\%$  of the maximal response size (type 1 responses) or whether increases were more graded (type 2 responses). We interpreted that cells in the first group would be innervated by one or few fibers, whereas those in the second group would be innervated by multiple fibers. In 55% (5 of 9) of stage 42/43 cells tested, the hindbrain-tectal projection was Type 1. As the animals develop, the percentage of type 1 responses decreased to 33% (3 of 9) by stage 44–46 and to 14% (1 of 7) by stage 48/49. This developmental increase in graded synaptic transmission indicates that the developing hindbrain-tectal projection is incorporating increasing numbers of fibers, which may convey increasingly varied mechanosensory information to tectal cells.

In the developing tectum, nascent excitatory retinotectal synapses express an increased quantal size, which decreases over development (Aizenman and Cline 2007; Pratt and Aizenman 2007). To test whether hindbrain-tectal synapses follow a similar developmental profile, we measured asynchronous EPSCs (aEPSCs) induced by hindbrain stimulation. aEPSCs can be evoked by substituting extracellular  $\text{Ca}^{2+}$  with  $\text{Sr}^{2+}$  (Xu-Friedman and Regehr 2000); see METHODS). This results in asynchronous synaptic release allowing EPSCs resulting from the release of single vesicles from the stimulated pathway to be resolved (Fig. 8A). This manipulation allowed us to analyze unitary synaptic events resulting from stimulation of an identified pathway. We found that the quantal size of the hindbrain-tectal projection did not significantly decrease in amplitude (pA) across the three developmental epochs investigated in this

study (Fig. 8C; 42/43:  $9.05 \pm 0.87$  pA,  $n = 13$ ; 44/46:  $8.25 \pm 0.97$  pA,  $n = 10$ ; 48/49:  $7.52 \pm 1.05$  pA,  $n = 8$ ;  $P > 0.05$ ).

Using this method we also directly compared the quantal size of hindbrain inputs and visual inputs to a given tectal neuron across development. We found that at all developmental stages, the quantal size of visual inputs was not significantly different from that of hindbrain inputs (Fig. 8, *B* and *E*). However, consistent with prior observations, the quantal size of visual inputs significantly decreased during this developmental time period (Fig. 8D; 42–43:  $11.03 \pm 0.987$  pA,  $n = 13$ ; 44–46:  $10.21 \pm 1.207$  pA,  $n = 10$ ; 48–49:  $6.71 \pm 0.786$  pA,  $n = 8$ ;  $P = 0.006$ ), in contrast to the lack of change observed in the quantal size of HB inputs. This result supports our earlier conclusion that the observed decrease of the A/N ratio between stages 44–46 and stage 48/49 is likely due to a new wave of synaptogenesis in hindbrain synapses because the difference cannot be accounted for by a decrease in the amplitude of AMPAR-mediated quantal events.

## DISCUSSION

Here we describe the development of mechanosensory projections to the optic tectum, which originate in primary sensory nuclei in the hindbrain. Our anatomical studies indicate that the hindbrain projection carries information from a variety of mechanosensory modalities likely originating from the trigeminal, facial, acousticovestibular, and lateral-line nerves. These projections terminate in an area of the hindbrain containing various primary sensory nuclei, including the dorsal column nucleus, dorsal medullary nucleus, and lateral line nucleus. The projection from the hindbrain to the tectum is present at least from developmental stage 42 and becomes more pronounced by stage 49. Furthermore, this projection overlaps in the same area of the

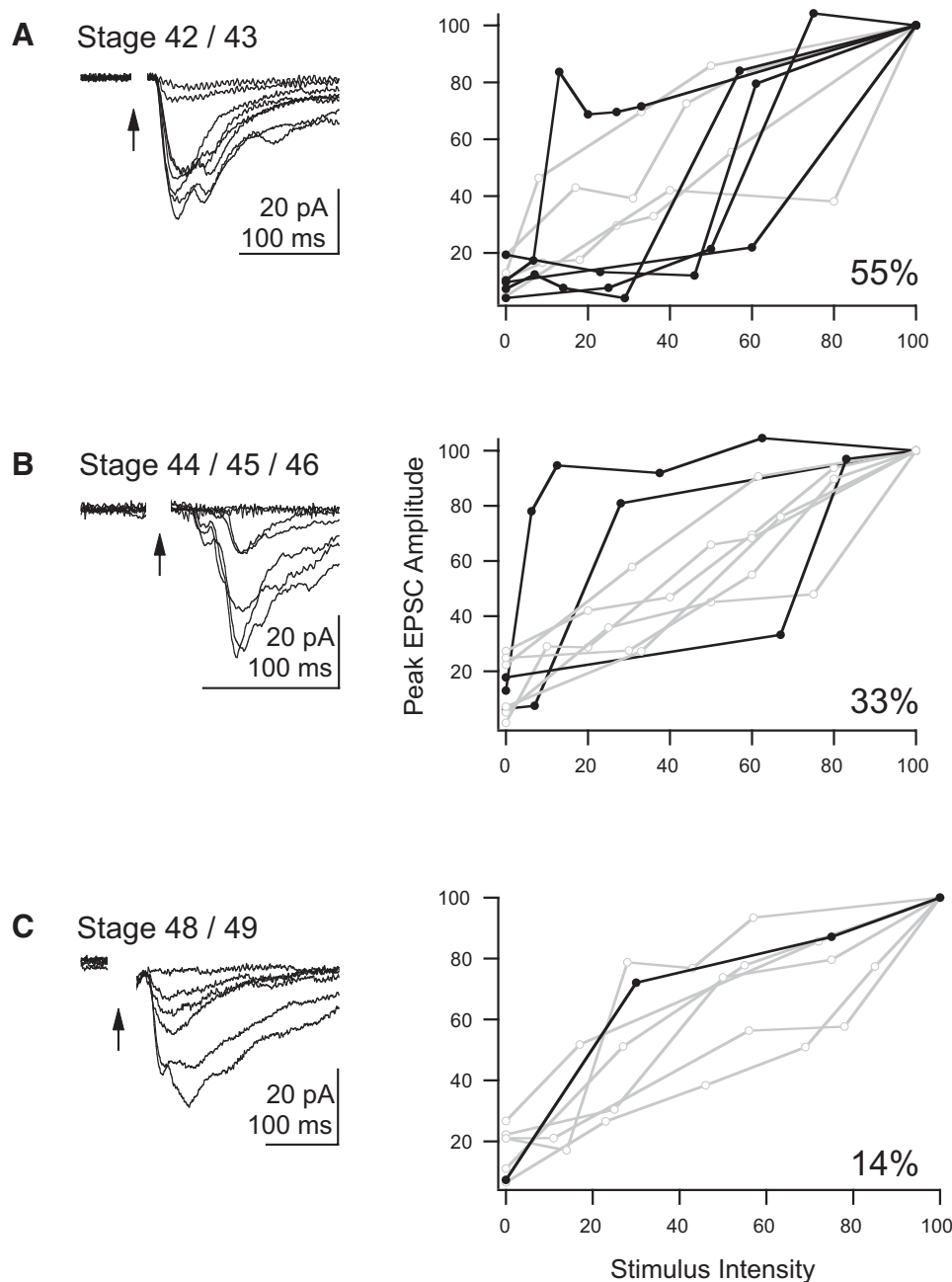


FIG. 7. Input/output curves indicate degree of convergence of hindbrain-tectal inputs. Each line represents data points from a single cell; the line graphs summarize the data across cells and animals. *A, left*: representative traces showing the effects of a gradual increase in stimulation intensity on response amplitude in a representative stage 42 neuron. *Right*: summary of peak EPSC amplitudes from each cell plotted against stimulus intensity. All values were normalized according to methods. Individual input-output curves were grouped according to whether they showed one "jump" in amplitude of  $\geq 65\%$  of the maximal response size (type 1 responses, black lines, closed circles), or whether increases were more graded (type 2 responses, gray lines, open circles). We interpreted that cells in the 1st group would be innervated by one or few fibers, whereas those in the second group would be innervated by multiple fibers. In 55% (5 of 9) of stage 42/43 cells tested, the hindbrain-tectal projection was type 1. *B* and *C*: same as *A* but for older tadpoles. As the animals develop, the percentage of type 1 responses decreased to 33% (3 of 9) by stage 44–46 and to 14% (1 of 7) by stage 48/49. This indicates that over development the number of hindbrain fibers innervating a given tectal cell increases.

tectal neuropil as retinotectal inputs, although it seems to terminate in more ventral regions of the tectum.

Functionally, hindbrain-tectal synapses are active during this time period and show no change in paired-pulse facilitation in contrast to visual inputs. Furthermore, the hindbrain inputs show a small, transient increase in AMPA/NMDA ratio between stages 42/3 and 44–46, and a significant decrease in this ratio by stages 48/9. This is also accompanied by electrophysiological evidence consistent with a developmental increase in the number of fibers innervating the tectum from the hindbrain, suggesting that the decrease in A/N ratio may be due to a large increase in the number of newly formed, immature synapses. The mechanosensory modalities thus appear to follow a different developmental profile than do visual inputs. Taken together, these data show that the tectum can integrate inputs from a variety of sensory modalities from very early on in

development, making this an attractive, experimentally tractable preparation with which to study the early development of multisensory integration at a cellular level.

#### *Comparison between the development of the retinotectal and mechanosensory projections*

Our data indicate that the developmental profile of mechanosensory hindbrain-tectal projections differs from that of the retinotectal projection in its level of facilitation, A/N ratio, and quantal size. The decrease in PPF at hindbrain-tectal synapses is small and nonsignificant unlike the large drop in PPF observed in the retinotectal projection between early and late stage tadpoles (Aizenman and Cline 2007). This decrease in PPF seen at hindbrain-tectal synapses is further distinguished from that seen at retinotectal synapses by the fact that retinotectal synapses never-



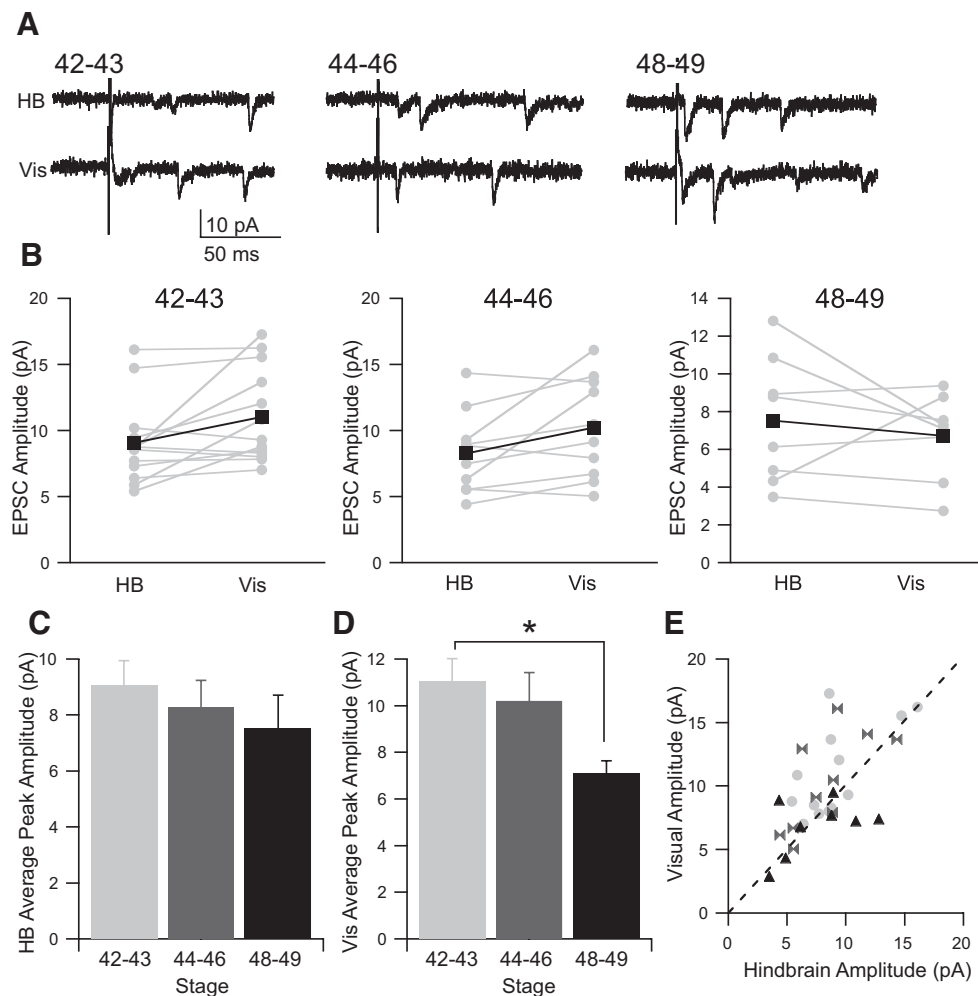


FIG. 8. Quantal size of evoked hindbrain and visual inputs to tectal neurons across development. *A*: representative traces of tectal responses to direct stimulation of the hindbrain (HB) or visual (Vis) projections in the presence of  $\text{Sr}^{2+}$ . *B*: asynchronous EPSC (aEPSC) amplitudes evoked by stimulation of different pathways that terminate on the same tectal cell are paired and connected by a line. The average evoked aEPSC amplitudes resulting from hindbrain and visual pathway stimulation are represented by black squares connected by a black line. We did not see consistent differences between aEPSC amplitudes of HB or Vis inputs to a given cell across development. *C*: average peak aEPSC amplitudes resulting from direct stimulation of the hindbrain across development (42–43:  $9.06 \pm 0.875$  pA,  $n = 13$ ; 44–46:  $8.25 \pm 0.97$  pA,  $n = 10$ ; 48–49:  $7.36 \pm 1.05$  pA,  $n = 8$ ). *D*: average aEPSC amplitudes resulting from direct stimulation of the visual inputs to tectal cells across development. The decrease in peak amplitude between stages 42–43 and 48–49 is significant (42–43:  $11.03 \pm 0.987$  pA,  $n = 13$ ; 44–46:  $10.21 \pm 1.207$  pA,  $n = 10$ ; 48–49:  $6.71 \pm 0.786$  pA,  $n = 8$ ;  $P = 0.006$ ). *E*: aEPSC amplitude evoked by visual stimulation plotted against aEPSC amplitude evoked by HB stimulation for each tectal neuron investigated from all 3 developmental epochs. Circles = 42–43; bow-ties = 44–46; triangles 48–49.

theless still facilitate in response to a paired pulse protocol at stage 48/49. Our data indicate that hindbrain tectal synapses neither facilitate nor depress at this stage, suggesting that their presynaptic release properties may ultimately develop differently than visual inputs.

The retinotectal projection matures by adding AMPAR to silent synapses accompanied by additional pruning of inputs that fail to mature (Cline and Haas 2008; Haas et al. 2006). Retinal ganglion cell axons first reach their target tectal cells by stage 39, and functional synapses that convey visual information are established by stage 42/43. The period between stage 44 and 46 is characterized by dramatic synaptogenesis. Highly motile retinal ganglion cell axon terminals synapse with the dynamic tectal cell dendritic arbor. By stage 48/49, AMPAR-mediated synaptic input increases as AMPAR are added to existing synapses (Akerman and Cline 2006), resulting in a significant increase in the A/N ratio between stage 42 and 49. Data from the retinotectal projection support a model whereby each axon from an individual retinal ganglion cell forms multiple synapses with each tectal neuron (Pratt and Aizenman 2007). As the retinotectal projection matures, the total number of retinal fibers carrying visual information to a given tectal cell decreases, while the number of mature synapses per-fiber increases.

We believe that the observed decrease in hindbrain-tectal AN ratio between stage 44–46 and 48/49 also underlies a wave

of synaptogenesis. One possibility is that these nascent hindbrain-tectal synapses are added as new fibers are recruited to the developing hindbrain-tectal projection. Thus the difference in A/N ratios between the hindbrain- and retinotectal projections could be due to a late wave of synaptogenesis on nascent hindbrain-tectal projections, resulting in a larger number of NMDAR-dominant silent synapses. This theory is supported by studies showing that nonvisual mechanosensory modalities restructure immediately preceding stage 48/49. Specifically, some aspects of lateral line system, believed to be important for rheotaxis, become functional at stage 47 (Simmons et al. 2004); although there is evidence that the lateral line system can function as early as stage 41 (Roberts et al. 2009). The inner ear of *Xenopus* tadpoles contains specific compartments to detect auditory, vestibular, and acoustico-vestibular stimuli. These compartments are established by stage 45. Between stage 45 and stage 50, morphological changes cause the ear to quadruple in length (Quick and Serrano 2005). Thus these studies show that major functional changes occur along the mechanosensory hindbrain-tectal projection during the same developmental time period in which we observe a significant decrease in A/N ratio.

One interesting contrast with mammals is that in the mammalian colliculus, mechanoreceptor input precedes visual input during development. Recordings from the colliculus of neonatal kittens show that neurons sensitive to auditory and somatic

stimuli develop a few days before the appearance of visual responses (Stein et al. 1973). This may facilitate orienting to and localizing the mother's nipple (Larson and Stein 1984). In contrast, neurons in the tadpole tectum appear to acquire visual responsivity either before or simultaneously with mechanosensory input. One possible reason might be the need for tadpoles to develop visually-guided behavior early in development to avoid predation and seek shelter (Dong et al. 2009).

A final point of distinction between retinotectal and hindbrain-tectal inputs can be found by examining the quantal size of the various inputs across development. It is known that the quantal size of visual inputs decreases across development (Pratt and Aizenman 2007). In contrast, the quantal size of hindbrain-tectal synapses remains relatively constant across the three developmental epochs examined here. These data further support our model of hindbrain-tectal development in which nascent synapses are continuously added to nascent fibers as opposed to a coordinated maturation of synapses in established retinotectal inputs.

Taken together, our data therefore support a hypothesis in which the hindbrain-tectal projection increasingly incorporates new fibers as the different mechanosensory modalities develop. These new fibers form nascent synapses that are immature and are characterized primarily by NMDAR. During the same developmental window, the retinotectal projection, in contrast, undergoes a period of refinement, where fibers are pruned and AMPAR are added to existing synapses, while the number of synapses each retinotectal axon makes increases. One important caveat in this hypothesis, however, is that because we are likely activating multiple mechanosensory modalities by directly stimulating the hindbrain, is also possible that different mechanosensory modalities may be following different developmental time courses, and this may confound the interpretation of the results.

#### Open questions and future directions

This study has characterized the development of mechanosensory inputs in vitro using direct electrical stimulation of a whole-brain preparation. This preparation has the important advantage that we can directly activate hindbrain inputs monosynaptically and thus are able to study changes in their synaptic properties. However, using our method, we cannot distinguish between the different mechanosensory modalities. It would be informative to expand this data by performing in vivo stimulation of the putative modalities carried by the hindbrain-tectal projections. An in vivo approach would allow us to directly stimulate the modalities composing the hindbrain-tectal projection individually. Using actual sensory stimuli to activate the auditory, lateral-line or somatosensory inputs in vivo across development will allow us to address the question of whether the relative "weight" of various mechanosensory inputs to tectal cells changes during this time period. It will also allow us to address the question of whether the different modalities in the hindbrain-tectal projection mature at different rates. Previous work in urodele amphibians has shown that there is a developmental sequence in the projection of sensory afferents to the hindbrain, from trigeminal, facial, inner ear, and finally lateral line (Fritzsche et al. 2005). This study supports the idea that the hindbrain-tectal projection may carry information from sepa-

rate sensory modalities at different developmental time periods.

In other species, different sensory modalities are known to influence each other during development (Knudsen 2002; Wallace and Stein 2007; Wallace et al. 2006). Our preparation would allow us to ask similar questions about whether the development of the hindbrain-tectal projection is instructed by the development of visual inputs. It has been demonstrated that visual experience plays instructive and permissive roles in the maturation of retinotectal synapses and refinement of the retinotectal map (Cline 1991; Debski and Cline 2002; Ruthazer and Cline 2004). Furthermore, visual activity is also important for guiding the alignment of the ipsilateral visual map from the nucleus isthmus with the contralateral retinotectal map (Udin and Grant 1999). It would be intriguing to know whether similar mechanisms are at play in the hindbrain input. For example, in the mature tectum, different populations of cells can be found that respond to either single sensory modalities or to different combinations (Behrend et al. 2006; Lowe 1987). In our study, we found that all cells that receive input from retinotectal synapses also receive hindbrain inputs. It would be interesting to know whether this is a transient phenomenon, in *Xenopus*, and whether this pattern changes during later developmental stages, and whether this process is activity dependent. For example, in mature *Xenopus*, cells residing in deeper tectal layers are unlikely to receive direct visual input. At which point in development do these cells lose visual input? Or do these cells develop later?

#### Conclusion

Here we have described the development of mechanosensory inputs to the optic tectum in *Xenopus* tadpoles. Our anatomical data indicate that the trigeminal ganglion and the nerve bundle that carries VIIth and VIIIth nerve and lateral-line inputs all project to primary sensory nuclei in the hindbrain. Nerve fibers from the hindbrain make monosynaptic connections with cells in the contralateral tectum. All tectal cells investigated in this study received input from both the contralateral hindbrain and retinotectal projections.

Our results have characterized for the first time the development of nonvisual inputs to tectal cells in the developing *X. laevis* tadpole. We have outlined important differences in the developmental time course of hindbrain-tectal and retinotectal synapses and established the developing *X. laevis* tadpole as an important model system with which to study bottom-up multisensory integration across development.

#### ACKNOWLEDGMENTS

We thank A. Simmons and H. Cline for helpful discussion and revisions of the manuscript.

#### GRANTS

This work was funded by the National Science Foundation (IOB) and the Klingenstein Fund. K. E. Deeg was supported by an institutional National Research Service Award from the National Institute of Mental Health.

#### REFERENCES

- Aizenman CD, Cline HT. Enhanced visual activity in vivo forms nascent synapses in the developing retinotectal projection. *J Neurophysiol* 97: 2949–2957, 2007.

- Akaneya Y, Altinbaev R, Bayazitov IT, Kinoshita S, Voronin LL, Tsumoto T. Low-frequency depression of synaptic responses recorded from rat visual cortex. *Neuroscience* 117: 305–320, 2003.
- Akerman CJ, Cline HT. Depolarizing GABAergic conductances regulate the balance of excitation to inhibition in the developing retinotectal circuit in vivo. *J Neurosci* 26: 5117–5130, 2006.
- Behrend O, Branoner F, Zhivkov Z, Ziehm U. Neural responses to water surface waves in the midbrain of the aquatic predator *Xenopus laevis laevis*. *Eur J Neurosci* 23: 729–744, 2006.
- Chahoud BH, Cordier-Picouet MJ, Clairambault P. Larval development of tectal efferents and afferents in *Xenopus laevis* (Amphibia Anura). *J Hirnforsch* 37: 519–535, 1996.
- Clements JD, Bekkers JM. Detection of spontaneous synaptic events with an optimally scaled template. *Biophys J* 73: 220–229, 1997.
- Cline HT. Activity-dependent plasticity in the visual systems of frogs and fish. *Trends Neurosci* 14: 104–111, 1991.
- Cline H, Haas K. The regulation of dendritic arbor development and plasticity by glutamatergic synaptic input: a review of the synaptotrophic hypothesis. *J Physiol* 586: 1509–1517, 2008.
- Cline HT, Wu G-Y, Malinow R. in vivo development of neuronal structure and function. *Cold Spring Harbor Symp Quant Biol* LXI: 95–104, 1997.
- Debski EA, Cline HT. Activity-dependent mapping in the retinotectal projection. *Curr Opin Neurobiol* 12: 93–99, 2002.
- Dong W, Lee RH, Xu H, Yang S, Pratt KG, Cao V, Song YK, Nurmikko A, Aizenman CD. Visual avoidance in *Xenopus* tadpoles is correlated with the maturation of visual responses in the optic tectum. *J Neurophysiol* 101: 803–815, 2009.
- Ewert JP. Neural correlates of key stimulus and releasing mechanism: a case study and two concepts. *Trends Neurosci* 20: 332–339, 1997.
- Fritzsch B, Gregory D, Rosa-Molinari E. The development of the hindbrain afferent projections in the axolotl: evidence for timing as a specific mechanism of afferent fiber sorting. *Zoology* 108: 297–306, 2005.
- Gasparini S, Saviane C, Voronin LL, Cherubini E. Silent synapses in the developing hippocampus: lack of functional AMPA receptors or low probability of glutamate release? *Proc Natl Acad Sci USA* 97: 9741–9746, 2000.
- Haas K, Li J, Cline HT. AMPA receptors regulate experience-dependent dendritic arbor growth in vivo. *Proc Natl Acad Sci USA* 103: 12127–12131, 2006.
- Hiramoto M, Cline HT. Convergence of the sensory inputs into *Xenopus* tadpole tectum. *Soc Neurosci Abstr* 723.718, 2008.
- Hiscock J, Straznicky C. Peripheral and central terminations of axons of the mesencephalic trigeminal neurons in *Xenopus*. *Neurosci Lett* 32: 235–240, 1982.
- Holt CE. A single-cell analysis of early retinal ganglion cell differentiation in *Xenopus*: from soma to axon tip. *J Neurosci* 9: 3123–3145, 1989.
- Ingle D. Behavioral correlates of central visual function in anurans. In: *Frog Neurobiology*, edited by Precht W, Llinás R. Berlin: Springer-Verlag, 1976, p. 435–451.
- Isaac JT, Crair MC, Nicoll RA, Malenka RC. Silent synapses during development of thalamocortical inputs. *Neuron* 18: 269–280, 1997.
- Knudsen EI. Instructed learning in the auditory localization pathway of the barn owl. *Nature* 417: 322–328, 2002.
- Larson MA, Stein BE. The use of tactile and olfactory cues in neonatal orientation and localization of the nipple. *Dev Psychobiol* 17: 423–436, 1984.
- Lazar G. The development of the optic tectum in *Xenopus laevis*: a Golgi study. *J Anat* 116: 347–355, 1973.
- Liao D, Hessler NA, Malinow R. Activation of postsynaptically silent synapses during pairing-induced LTP in CA1 region of hippocampal slice. *Nature* 375: 400–404, 1995.
- Lowe DA. Organisation of lateral line and auditory areas in the midbrain of *Xenopus laevis*. *J Comp Neurol* 245: 498–513, 1986.
- Lowe DA. Single-unit study of lateral line cells in the optic tectum of *Xenopus laevis*: evidence for bimodal lateral line/optic units. *J Comp Neurol* 257: 396–404, 1987.
- Lowe DA, Russell IJ. The relation between soma position and fibre trajectory of neurons in the mesencephalic trigeminal nucleus of *Xenopus laevis*. *Proc R Soc Lond B Biol Sci* 221: 437–454, 1984.
- Munoz A, Munoz M, Gonzalez A, Ten Donkelaar HJ. Anuran dorsal column nucleus: organization, immunohistochemical characterization, and fiber connections in *Rana perezi* and *Xenopus laevis*. *J Comp Neurol* 363: 197–220, 1995.
- Nieuwkoop PD, Faber J. *Normal Table of Xenopus laevis* (Daudin). New York: Garland, 1956.
- Pratt KG, Aizenman CD. Homeostatic regulation of intrinsic excitability and synaptic transmission in a developing visual circuit. *J Neurosci* 27: 8268–8277, 2007.
- Pratt KG, Aizenman CD. Multisensory integration in mesencephalic trigeminal neurons in *Xenopus* tadpoles. *J Neurophysiol* 102: 399–412, 2009.
- Pratt KG, Dong W, Aizenman CD. Development and spike timing-dependent plasticity of recurrent excitation in the *Xenopus* optic tectum. *Nat Neurosci* 11: 467–475, 2008.
- Quick QA, Serrano EE. Inner ear formation during the early larval development of *Xenopus laevis*. *Dev Dyn* 234: 791–801, 2005.
- Roberts A, Feetham B, Pajak M, Teare T. Responses of hatchling *Xenopus* tadpoles to water currents: first function of lateral line receptors without cupulae. *J Exp Biol* 212: 914–921, 2009.
- Ruthazer ES, Akerman CJ, Cline HT. Control of axon branch dynamics by correlated activity in vivo. *Science* 301: 66–70, 2003.
- Ruthazer ES, Cline HT. Insights into activity-dependent map formation from the retinotectal system: a middle-of-the-brain perspective. *J Neurobiol* 59: 134–146, 2004.
- Simmons AM, Costa LM, Gerstein HB. Lateral line-mediated rheotactic behavior in tadpoles of the African clawed frog (*Xenopus laevis*). *J Comp Physiol A Neuroethol Sens Neural Behav Physiol* 190: 747–758, 2004.
- Stein BE, Labos E, Kruger L. Sequence of changes in properties of neurons of superior colliculus of the kitten during maturation. *J Neurophysiol* 36: 667–679, 1973.
- Stein BE, Stanford TR, Rowland BA. The neural basis of multisensory integration in the midbrain: its organization and maturation. *Hear Res* In press.
- Székely G, Lázár G. Cellular and synaptic architecture of the optic tectum. In: *Frog Neurobiology*, edited by Llinás R, Precht W. Berlin: Springer-Verlag, 1976, p. 407–434.
- Tao HW, Poo MM. Activity-dependent matching of excitatory and inhibitory inputs during refinement of visual receptive fields. *Neuron* 45: 829–836, 2005.
- Thomson AM. Facilitation, augmentation and potentiation at central synapses. *Trends Neurosci* 23: 305–312, 2000.
- Tsurudome K, Li X, Matsumoto N. Intracellular and current source density analyses of somatosensory input to the optic tectum of the frog. *Brain Res* 1064: 32–41, 2005.
- Udin SB, Grant S. Plasticity in the tectum of *Xenopus laevis*: binocular maps. *Prog Neurobiol* 59: 81–106, 1999.
- Vanegas H. *Comparative Neurology of the Optic Tectum*. New York: Plenum, 1984.
- Wallace MT, Carriere BN, Perrault TJ Jr, Vaughan JW, Stein BE. The development of cortical multisensory integration. *J Neurosci* 26: 11844–11849, 2006.
- Wallace MT, Stein BE. Early experience determines how the senses will interact. *J Neurophysiol* 97: 921–926, 2007.
- Will U, Luhede G, Görner P. The area octavo-lateralis in *Xenopus laevis*. I. The primary afferent projections. *Cell Tissue Res* 239: 147–161, 1985a.
- Will U, Luhede G, Görner P. The area octavo-lateralis in *Xenopus laevis*. II. Second order projections and cytoarchitecture. *Cell Tissue Res* 239: 163–175, 1985b.
- Wu GY, Cline HT. Stabilization of dendritic arbor structure in vivo by CaMKII. *Science* 279: 222–226, 1998.
- Wu GY, Cline HT. Time-lapse in vivo imaging of the morphological development of *Xenopus* optic tectal interneurons. *J Comp Neurol* 459: 392–406, 2003.
- Wu G, Malinow R, Cline HT. Maturation of a central glutamatergic synapse. *Science* 274: 972–976, 1996.
- Xu-Friedman MA, Regehr WG. Probing fundamental aspects of synaptic transmission with strontium. *J Neurosci* 20: 4414–4422, 2000.
- Zhang LI, Tao HW, Holt CE, Harris WA, Poo M. A critical window for cooperation and competition among developing retinotectal synapses. *Nature* 395: 37–44, 1998.
- Zittlau KE, Claas B, Munz H. Horseradish peroxidase study of tectal afferents in *Xenopus laevis* with special emphasis on their relationship to the lateral-line system. *Brain Behav Evol* 32: 208–219, 1988.
- Zou D-J, Cline HT. Coordinated regulation of retinal axon and tectal cell growth by endogenous CaMKII in vivo. *J Neurosci* 19: 8909–8918, 1999.